Gaseous Organometallics

DOI: 10.1002/anie.201201959

A Combined Gas-Phase Photoelectron Spectroscopic and Theoretical Study of Zeise's Anion and Its Bromine and Iodine Analogues**

Gao-Lei Hou, Hui Wen, Kenneth Lopata, Wei-Jun Zheng, Karol Kowalski, Niranjan Govind, Xue-Bin Wang, and Sotiris S. Xantheas**

Zeise's salt, potassium trichloro(ethylene)platinate(II), with the formula $K[PtCl_3(C_2H_4)]\cdot H_2O$, has long been known as the first organometallic compound. The salt was named after its inventor, William Christopher Zeise, who reported its synthesis in the 1820s.[1] The chemical bonding and molecular structure of this compound remained largely unknown and was intensely debated[2] for over a hundred years until the 1950s, when the Dewar–Chatt–Duncanson (DCD) model[3,4] was introduced. According to that model, a normal molecular dative bond involving the overlap between the filled ethylene π orbital and an empty Pt $5d6s6p^2$ orbital forms a σ bond, which is reinforced by back-bonding that involves the Pt donating electrons from the filled 5d6p orbital back to the empty ethylene π^* anti-bonding orbital, yielding a cooperative π^* anti-bond. Such a bonding scheme would require the ethylene to be oriented perpendicularly to the $PtCl_3$ plane, forming an η^2 ethylene ligand. This structural arrangement was confirmed by X-ray and neutron diffraction studies in the 1970s,[5,6] 150 years after the original discovery of the platinum-ethylene complex. Many experimental studies have been conducted to probe the structure and bonding of Zeise's salt, including X-ray and neutron diffraction,[5,6] vibrational spectroscopy,[4,7–9] and ultraviolet solution absorption spectroscopy.[10–12] The ethylene ligand symmetrically interacts with the Pt atom, with the C–C axis being perpendicular to the $PtCl_3$ plane. The three Pt–Cl bonds are not all equal, with the *trans* bond being slightly longer. The C–C distance is approximately 4% longer than the corresponding one in free ethylene, with the four C–H bonds bent away from the Pt atom.[6] The C–C stretching frequency is also red-shifted.[7–9] These findings can be qualitatively explained by the DCD bonding model,[3,4] and have been essentially confirmed by earlier molecular orbital calculations[13,14] and related theoretical studies.[15–20]

Besides being a historically key species in the field of organometallic chemistry in defining new chemical concepts (such as hapticity) and modes of chemical bonding, Zeise's salt and its dimer have also been found to be effective in many important catalytic processes,[21–23] as well as being used as versatile chiral derivatizing agents in asymmetric synthesis.[24,25] The Br analogue of Zeise's salt is an important intermediate and was shown to activate the hydroamination of ethylene.[26,27] The accurate description and detailed electronic structural information on Zeise's complex, especially the degree of activation of the complexed ethylene, relate directly to the reactivity of the complex towards nucleophilic species in various homogeneous catalytic processes.[28]

To date, all experimental data on Zeise's anion and the Br analogue of the complex have been reported in the condensed phase, a fact that often prevents detailed characterization because of complications that arise from solvation, counter ions, and crystal packing. There have also been no results reported thus far for the I analogue. A gas phase study is therefore highly desirable to unravel the subtle properties of the isolated Zeise's species and the trends involving its heavier halogen analogues without the complications of the condensed phase environment.

As has been previously shown, gas-phase anion photoelectron spectroscopy (PES), when combined with accurate gas-phase electronic structure calculations, represents a powerful approach for probing the electronic structure and bonding properties of isolated metal complexes.[29,30] Herein, we present a combined experimental and theoretical study of Zeise's anion and its Br and I analogues.

Figure 1 shows the $T = 20$ K PES spectra of $[PtX_3(C_2H_4)]^-$ (X = Cl, Br, I) at 193 (blue) and 157 nm (red). A wealth of well-resolved sharp features corresponding to electronic transitions from the ground state of the anion to the ground and excited states of the corresponding neutral species are observed for each species, yielding unprecedented electronic structure information for the neutral species. Within the single particle framework (Koopmans' approximation), these observed spectral features can be viewed as originating from

[*] G.-L. Hou, H. Wen, Dr. X.-B. Wang, Dr. S. S. Xantheas
Chemical & Materials Sciences Division
Pacific Northwest National Laboratory
P.O. Box 999, Richland, Washington 99352 (USA)
E-mail: xuebin.wang@pnnl.gov
sotiris.xantheas@pnnl.gov

G.-L. Hou, Dr. W.-J. Zheng
Beijing National Laboratory for Molecular Sciences, State Key Laboratory of Molecular Reaction Dynamics, Institute of Chemistry
Chinese Academy of Sciences, Beijing 100190 (China)

Dr. K. Lopata, Dr. K. Kowalski, Dr. N. Govind
Environmental Molecular Sciences Laboratory
Pacific Northwest National Laboratory
P. O. Box 999, Richland, Washington 99352 (USA)

[**] This work was supported by the Division of Chemical Sciences, Geosciences, and Biosciences, Office of Basic Energy Sciences, U.S. Department of Energy (DOE). Part of this work was performed at the Environmental Molecular Sciences Laboratory (EMSL), a national scientific user facility sponsored by DOE's Office of Biological and Environmental Research and located at Pacific Northwest National Laboratory, which is operated by Battelle Memorial Institute for the DOE. K.L. acknowledges the Wiley Postdoctoral fellowship from EMSL.

Supporting information for this article is available on the WWW under http://dx.doi.org/10.1002/anie.201201959.

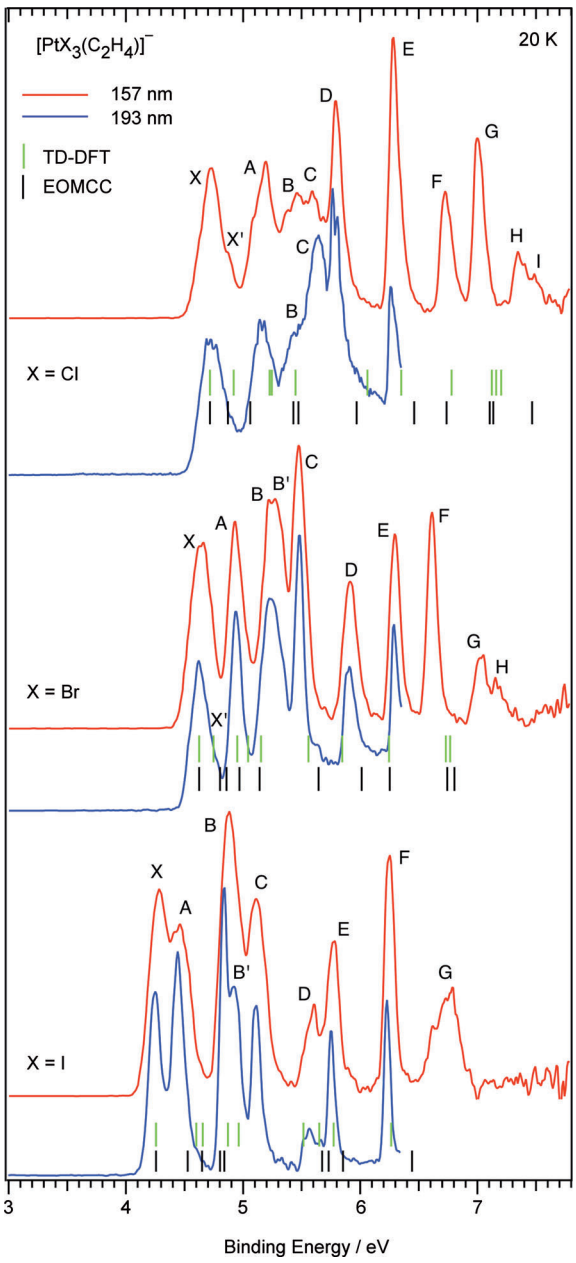

Figure 1. The 193 (6.424 eV, ——) and 157 nm (7.867 eV, ——) photoelectron spectra of $[PtX_3(C_2H_4)]^-$ at $T = 20$ K. Short vertical bars denote the excited states of the neutrals, as calculated with TDDFT (|) and CR-EOMCCSD(T) (||).

Table 1: Observed and calculated vertical (VDE) and adiabatic (ADE) detachment energies for $[PtX_3(C_2H_4)]^-$ (X = Cl, Br, I) and state assignments.

X	ADE [eV] Exp.[a] Calc.[b,c]		VDE [eV] Exp.[d]	ΔE-exp.[e]	TD-DFT	CR-EOMCCSD(T)
Cl	4.57(2)[a]	X	4.72(2)	0	0	0
	[4.45][b]	X′	4.86(5)	0.14	0.20 (B_1)	0.15 (B_1)
	(4.44)[c]	A	5.17(2)	0.45	0.52(B_2)	0.35 (A_1)
		B	5.45(5)	0.73	0.52 (A_1)	0.71 (B_1)
		C	5.61(2)	0.89	0.73 (B_1)	0.75 (B_2)
		D	5.77(2)	1.05	1.35 (A_1)	1.26 (A_1)
		E	6.27(2)	1.55	1.63 (B_2)	1.74 (B_2)
		F	6.72(2)	2.00	2.06 (B_1)	2.00 (B_1)
		G	7.00(2)	2.28	2.41 (A_1)	2.38 (A_2)
		H	7.34(5)	2.62	2.45 (B_2)	2.41 (A_1)
		I	7.48 (5)	2.76	2.48 (A_2)	2.75 (B_2)
Br	4.51(2)[a]	X	4.63(2)	0	0	0
	[4.40][b]	X′			0.12 (B_1)	0.17 (B_1)
	(4.39)[c]	A	4.92(2)	0.29	0.31 (B_2)	0.21 (B_1)
		B	5.22(2)	0.59	0.40 (B_1)	0.34 (A_1)
		B′	5.32(5)	0.69	0.51 (A_1)	0.50 (B_2)
		C	5.47(2)	0.84	1.05 (A_1)	1.03 (A_1)
		D	5.90(2)	1.27	1.21 (B_2)	1.39 (B_2)
		E	6.28(2)	1.65	1.60 (B_1)	1.62 (B_1)
		F	6.62(2)	1.99	2.10 (A_1)	2.12 (A_2)
		G	7.04(2)	2.41	2.12 (A_2)	2.17 (A_1)
		H	7.16(2)	2.53		
I	4.18(2)[a]	X	4.27(2)	0	0	0
	[4.25][b]	A	4.45(2)	0.18	0.33 (A_2)	0.25 (A_2)
	(4.11)[c]	B	4.86(2)	0.59	0.37 (B_2)	0.37 (B_2)
		B′	4.92(2)	0.65	0.61 (A_1)	0.54 (A_1)
		C	5.10(2)	0.83	0.69 (B_1)	0.56 (B_1)
		D	5.59(2)	1.32	1.24 (B_2)	1.42 (B_2)
		E	5.78 2)	1.51	1.38 (A_1)	1.45 (A_1)
		F	6.24(2)	1.97	1.50 (B_1)	1.58 (B_1)
		G	6.75(5)	2.48	2.00 (B_2)	2.19 (A_1)

[a] Estimated by a straight line at the leading edge of the ground state transition and adding a constant (2.5% of the kinetic energy of the detached electrons as calibrated using the second I^- peak (4.002 eV) at the same conditions) to the intercept with the binding energy axis to account for the resolution of the instrument. These also represent the electron affinity of the neutral $[PtX_3(C_2H_4)]$. [b] Calculated energy difference between the anion and neutral species at their respective optimized geometries with B3LYP (including zero-point corrections) [c] Includes spin-orbital splitting. [d] Measured from the peak maxima. [e] VDE differences relative to VDE (X) (first peak).

the detachment of electrons from the occupied molecular orbitals of the anion, thus directly reflecting the chemical interactions and bonding of Zeise's anion and its analogues.

The adiabatic detachment energy (ADE) of the anion $[PtX_3(C_2H_4)]^-$, measured from the onset threshold of each spectra, is relatively high and decreases with halogen size: 4.57 (Cl), 4.51 (Br), and 4.18 eV (I) (Table 1). The observed vertical detachment energies (VDEs), determined from the peak maxima, represent the transitions from the ground state of the anion to the ground and excited states of the neutral species at the anion's geometry, and are also listed in Table 1.

A single vibrational progression was discernibly resolved for the ground state (X) and two excited state (A, D) transitions of $[PtCl_3(C_2H_4)]^-$ at 193 nm, both with a frequency of $[320 \pm 20]$ cm^{-1} (Figure 2). However, no similar structure was observed for the Br and I analogues. According to the reported vibrational frequencies obtained from the solid-state and solution-phase studies,[7] both the Pt–C_2 and the Pt–Cl symmetric stretching of the anion have frequencies in that range. The observation that only the spectrum of the Cl analogue exhibits this vibrational fine structure suggests that the observed vibrational excitation is due to the symmetric Pt–Cl stretching in the neutral potential energy surface and, in turn, implies that the highest occupied molecular orbital (HOMO) of $[PtCl_3(C_2H_4)]^-$ mainly consists of the $PtCl_3$

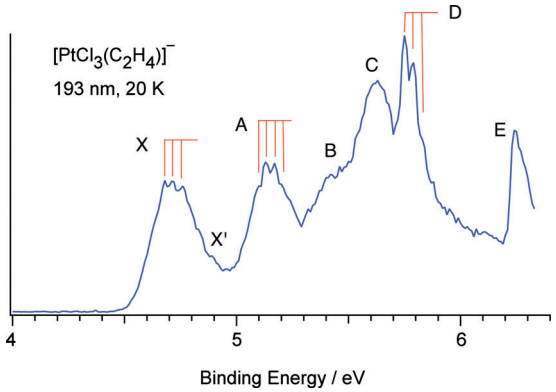

Figure 2. The 193 nm photoelectron spectrum of $[PtCl_3(C_2H_4)]^-$ at $T = 20$ K, showing vibrational progressions in the ground (X) and two excited states (A, D), both with a frequency of $[320 \pm 20]$ cm^{-1}.

moiety, a fact that is confirmed by the theoretical analysis (see below).

The geometries of both the anions and the neutrals, optimized without any symmetry restrictions, converged to the familiar bonding picture in which the linear ethylene ligand interacts perpendicularly with the mostly planar PtX_3^- moiety to form a dative (η^2) bond (Supporting Information, Figure S1). The C=C bond of ethylene is significantly elongated compared to that of free C_2H_4 (1.339 Å), with the *trans* Pt–X bond length being longer than the *cis* bond for all species. The binding energy between C_2H_4 and PtX_3^- is found (at the DFT/B3LYP level) to decrease monotonically with halide ligand size: 1.54, 1.37, and 1.10 eV for the Cl, Br, and I species, respectively. This trend is consistent with the fact that the Cl analogue was the first one synthesized, whereas the I species had not been reported prior to our study. The weaker interaction between $PtBr_3^-$ and C_2H_4 also provides an explanation of why the Br analogue is more reactive than the Cl analogue in several catalytic processes.[26,27] The calculated ADEs, including spin-orbit effects, lie within 0.1 eV of the experimentally measured ones, and they exhibit the observed decreasing trend. Spin-orbit effects have a marginal effect on the Cl and Br species, whereas they are stronger for the I species. (Table 1).

It is challenging to accurately describe the excited states of open-shell species, in particular those involving 5d transition metals, where a delicate treatment of electron correlation and possibly multi-reference character are essential. The calculated excitation energies were found to be in good agreement with the experimentally determined ones for both the time-dependent density functional theory (TD-DFT) and equation-of-motion coupled cluster (EOMCC) methods (Table 1). Although all excited states listed in Table 1 are dominated by single excitations from the ground state, they all have strong multi-reference character. The calculated excitation energies (vertical bars) are listed with respect to the first VDE of each species, and compared with the observed ones, as shown in Figure 1 and Table 1. The TD-DFT and EOMCC stick spectra yield a similar spectral pattern and are in good overall agreement with experiment. Five closely spaced electronic states exist in the low binding energy region for each anion: X, X′, A, B, C for the Cl species; X, X′, A, B, B′ for the Br species; and X, A, B, B′, C for the I species. These are followed by an energy gap and a few relatively separated peaks at higher energies.

Shining light on Zeise's anion results in detaching the excess electron from the highest occupied molecular orbitals (MOs), which define the nature of the chemical bonding for each species. The rich and well-resolved spectrum (Figure 1) provides a means of probing the chemical bonding and electronic structure for this important class of molecules. Our MO analysis reveals that the highest occupied MOs for Zeise's anion and its counterparts are localized within PtX_3 (see MO composition percentages in Figure 3), whereas deeply bound MOs have significant contributions from both $PtCl_3$ and C_2H_4 in line with the DCD model (Supporting Information, Figure S2), and consistent with previous theoretical studies.[14,17] The vibrationally resolved $[PtCl_3(C_2H_4)]^-$ spectrum (Figure 2) further supports the aforementioned MO analysis: the first two features (X and A) are relatively broad, with a long vibrational progression owing to excitation of the Pt–Cl stretching with a calculated frequency of 363 cm^{-1} (B3LYP/aug-cc-pVTZ). The observed trend in the ADEs also indicates that the HOMO of this class of anions arises

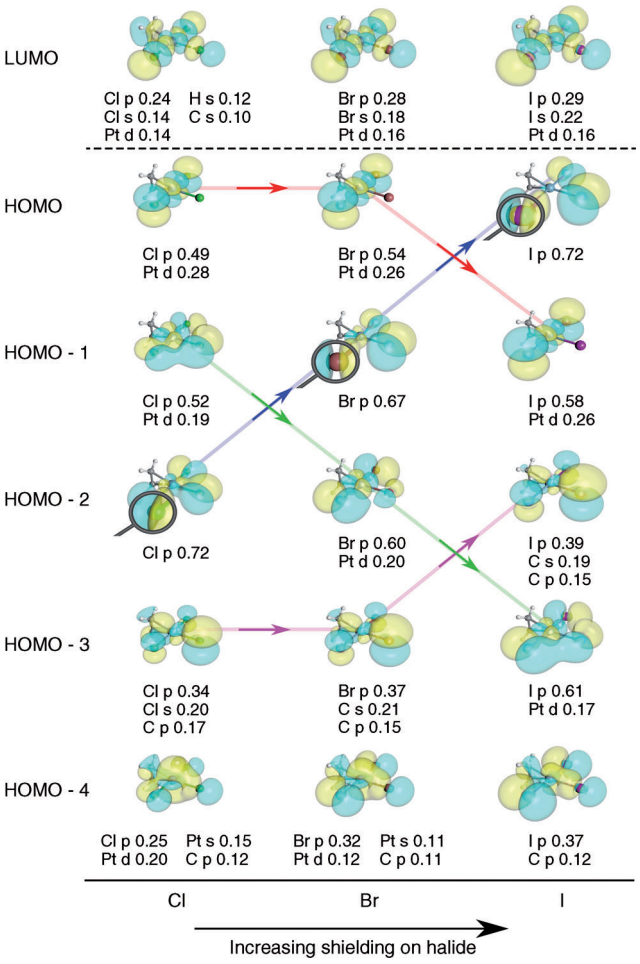

Figure 3. Frontier MOs of $[PtX_3(C_2H_4)]^-$, demonstrating how increased shielding on the halide ligand affects the MO ordering. The dominant (>10%) atomic orbital contributions are indicated for each case.

mainly from the contribution of PtX_3^- and the decreased ADE for the heavy halogen species is primarily due to the lower ADE of the corresponding halide. An interesting reordering of frontier MOs is observed from our calculations, as indicated by the arrows in Figure 3. Going down the series, there is a reordering of some of the MOs, largely owing to increased shielding of the heavier halide atoms (see magnified atoms). This results in more diffuse orbitals, an effect that in turn stabilizes bonding-like orbitals and destabilizes anti-bonding-like ones.

In conclusion, the activation of olefins by transition metals is a key process that is important to many homogeneous catalytic reactions, for which significant ligand substitution effects have been observed. Both the electron binding and the interaction energies of ethylene with platinum tri-halide are observed to decrease with halide size, a fact that is consistent with stronger shielding. We believe that our results can serve as a benchmark for a fundamental understanding of the interactions in this class of compounds and enhance our understanding beyond the DCD model description.

Experimental Section

The PES experiment was performed using a low-temperature ESI source PES apparatus, the details of which were recently published.[31] The gaseous Zeise's anion, $[PtCl_3(C_2H_4)]^-$, was readily produced by spraying a ca. 10^{-4} M acetonitrile/water (3:1 volume ratio) solution of $K[PtCl_3(C_2H_4)]\cdot H_2O$, whereas the Br and I analogues were obtained by halide ligand exchange from Zeise's salt mixed with KBr or NaI. However, the same procedure using KF failed to produce the F analogue, $[PtF_3(C_2H_4)]^-$. All anions produced were guided by two RF-only quadrupoles and a 90° bender into a cryogenically controlled ion trap, where they were accumulated and cooled by collisions with a buffer gas of ca. 0.1 mTorr (20% H_2 balanced with helium) for 20–80 ms, before being pulsed out into the extraction zone of a time-of-flight mass spectrometer with a 10 Hz repetition rate. All ions were pre-cooled to 20 K. The low temperature serves to eliminate hot bands in the spectrum.

For each PES experiment, the desired anions were first mass selected and decelerated before being intercepted by a probe laser beam in the photodetachment zone of a magnetic bottle photoelectron analyzer. In the current experiment, light at both 193 nm (6.424 eV) from an ArF excimer laser and at 157 nm (7.867 eV) from an F_2 laser was used. The laser was operated at a 20 Hz repetition rate with the ion beam off at alternating laser shots for shot-by-shot background subtraction. Photoelectrons were collected at nearly 100% efficiency by the magnetic bottle and analyzed in a 5.2 m long electron flight tube. Time-of-flight photoelectron spectra were collected and converted to kinetic energy spectra, and calibrated by the known spectra of I^- and $[Cu(CN)_2]^-$. The electron binding energy spectra were obtained by subtracting the kinetic energy spectra from the detachment photon energy. The electron energy resolution ($\Delta E/E$) was about 2%, which amounts to ca. 20 meV for 1 eV electrons.

Theoretical Details

All calculations were performed with the NWChem computational chemistry suite.[32,33] We have carried out excited state calculations using time-dependent density functional theory (TD-DFT) and the equation-of-motion coupled cluster (EOMCC) method.[34] In the latter case, we employed the completely renormalized EOMCCSD(T) (CR-EOMCCSD(T)) approach, which perturbatively includes the effect of triply excited configurations.[35,36] For the ground-state DFT calculations, all geometries were optimized using the B3LYP exchange-correlation functional.[37] The excited-state TD-DFT calculations were performed using the CAM-B3LYP[38] functional. The attenuation parameter (γ) was set to 0.33, which has been previously shown to yield excitation energies that are in excellent agreement with high-level coupled-cluster (CC) calculations.[36] All DFT and CC calculations for C, H, Cl, and Br atoms were performed with the aug-cc-pVTZ basis set.[39] For I atoms, the aug-cc-pVTZ-PP basis set with the Stuttgart–Köln MCDHF RSC ECP (28 core electrons)[40] was used. For Pt atoms, the (8s,7p,6d)→[6s,5p,3d] basis set,[41] in conjunction with the Stuttgart–Köln MCDHF RSC ECP (60 core electrons)[40] was used. Spin-orbit effects were estimated using the CRENBL ECP.[42] All ECPs and basis sets were obtained from the EMSL Basis Set Exchange.[43]

Received: March 12, 2012
Published online: May 8, 2012

Keywords: ab initio calculations · excited states · organometallic compounds · photoelectron spectroscopy · Zeise's anion

[1] a) W. C. Zeise, *Poggendorff's Ann. Phys.* **1827**, *9*, 632; b) W. C. Zeise, *Poggendorff's Ann. Phys.* **1831**, *21*, 497–541; c) W. C. Zeise, *Pogg. Ann. Phys.* **1831**, *21*, 542–549; d) W. C. Zeise, *Poggendorff's Ann. Phys.* **1837**, *40*, 234.
[2] D. Seyferth, *Organometallics* **2001**, *20*, 2–6.
[3] M. J. S. Dewar, *Bull. Soc. Chim. Fr.* **1951**, *18*, C71–C79.
[4] J. Chatt, L. A. Duncanson, *J. Chem. Soc.* **1953**, 2939–2947.
[5] a) M. Black, R. H. B. Mais, P. G. Owston, *Acta Crystallogr. Sect. B* **1969**, *25*, 1753–1759; b) J. A. J. Jarvis, B. T. Kilbourn, P. G. Owston, *Acta Crystallogr. Sect. B* **1971**, *27*, 366–372.
[6] R. A. Love, T. F. Koetzle, G. J. B. Williams, L. C. Andrews, R. Bau, *Inorg. Chem.* **1975**, *14*, 2653–2657.
[7] J. Hiraishi, *Spectrochim. Acta Part A* **1969**, *25*, 749–760.
[8] J. A. Baldwin, D. F. R. Gilson, I. S. Butler, *J. Organomet. Chem.* **2005**, *690*, 3165–3168.
[9] P. A. Dub, O. A. Filippov, N. V. Belkova, M. Rodriguez-Zubiri, R. Poli, *J. Phys. Chem. A* **2009**, *113*, 6348–6355.
[10] R. G. Denning, F. R. Hartley, L. M. Venanzi, *J. Chem. Soc. A* **1967**, 1322–1325.
[11] T.-H. Chang, J. I. Zink, *J. Am. Chem. Soc.* **1984**, *106*, 287–292.
[12] H.-R. C. Jaw, T.-H. Chang, J. I. Zink, *Inorg. Chem.* **1987**, *26*, 4204–4208.
[13] J. W. Moore, *Acta Chem. Scand.* **1966**, *20*, 1154–1162.
[14] T. A. Albright, R. Hoffmann, J. C. Thibeault, D. L. Thorn, *J. Am. Chem. Soc.* **1979**, *101*, 3801–3812.
[15] P. J. Hay, *J. Am. Chem. Soc.* **1981**, *103*, 1390–1393.
[16] S. Sakaki, M. Ieki, *Inorg. Chem.* **1991**, *30*, 4218–4224.
[17] N. Rösch, R. P. Messmer, K. H. Johnson, *J. Am. Chem. Soc.* **1974**, *96*, 3855–3860.
[18] S. Strömberg, M. Svensson, K. Zetterberg, *Organometallics* **1997**, *16*, 3165–3168.
[19] J. Forniés, A. Martín, L. F. Martín, B. Menjón, *Organometallics* **2005**, *24*, 3539–3546.
[20] A. Ikeda, Y. Nakao, H, Sato, S. Sakaki, *J. Phys. Chem. A* **2007**, *111*, 7124–7132.
[21] K. Ikura, I. Ryu, N. Kanube, N. Sonoda, *J. Am. Chem. Soc.* **1992**, *114*, 1520–1521.
[22] J. Beyer, R. Madsen, *J. Am. Chem. Soc.* **1998**, *120*, 12137–12138.
[23] J. Beyer, P. R. Skaanderup, R. Madsen, *J. Am. Chem. Soc.* **2000**, *122*, 9575–9583.
[24] D. Parker, *Chem. Rev.* **1991**, *91*, 1441–1457.
[25] G. Uccello-Barretta, R. Bernardini, R. Lazzaroni, P. Salvadori, *Org. Lett.* **2000**, *2*, 1795–1798.
[26] J. J. Brunet, M. Cadena, N. C. Chu, O. Diallo, K. Jacob, E. Mothers, *Organometallics* **2004**, *23*, 1264–1268.

[27] P. A. Dub, R. Poli, *J. Am. Chem. Soc.* **2010**, *132*, 13799 – 13812.
[28] O. Eisenstein, R. Hoffmann, *J. Am. Chem. Soc.* **1981**, *103*, 4308 – 4320.
[29] X. B. Wang, L. S. Wang, *J. Am. Chem. Soc.* **2000**, *122*, 2339 – 2345.
[30] X. B. Wang, Y. L. Wang, J. Yang, X. P. Xing, J. Li, L. S. Wang, *J. Am. Chem. Soc.* **2009**, *131*, 16368 – 16369.
[31] X. B. Wang, L. S. Wang, *Rev. Sci. Instrum.* **2008**, *79*, 073108.
[32] M. Valiev, E. J. Bylaska, N. Govind, K. Kowalski, T. P. Straatsma, H. J. J. van Dam, D. Wang, E. Nieplocha, T. L. Win-dus, W. A. de Jong, *Comput. Phys. Commun.* **2010**, *181*, 1477 – 1489.
[33] NWChem: http://www.nwchem-sw.org.
[34] J. Geertsen, M. Rittby, R. J. Bartlett, *Chem. Phys. Lett.* **1989**, *164*, 57 – 62.
[35] K. Kowalski, P. Piecuch, *J. Chem. Phys.* **2004**, *120*, 1715 – 1738.
[36] K. Kowalski, S. Krishnamoorthy, O. Villa, J. R. Hammond, N. Govind, *J. Chem. Phys.* **2010**, *132*, 154103.
[37] P. J. Stephens, F. J. Devlin, C. F. Chabalowski, M. J. Frisch, *J. Phys. Chem.* **1994**, *98*, 11623 – 11627.
[38] T. Yanai, D. P. Tew, N. C. Handy, *Chem. Phys. Lett.* **2004**, *393*, 51 – 57.
[39] a) T. H. Dunning, Jr., *J. Chem. Phys.* **1989**, *90*, 1007 – 1023; b) R. A. Kendall, T. H. Dunning, Jr., R. J. Harrison, *J. Chem. Phys.* **1992**, *96*, 6796 – 6806.
[40] K. A. Peterson, D. Figgen, E. Goll, H. Stoll, M. Dolg, *J. Chem. Phys.* **2003**, *119*, 11113 – 11123.
[41] D. Andrae, U. Haeussermann, M. Dolg, H. Stoll, H. Preuss, *Theor. Chim. Acta* **1990**, *77*, 123 – 141.
[42] L. A. LaJohn, P. A. Christiansen, R. B. Ross, T. Atashroo, W. C. Ermler, *J. Chem. Phys.* **1987**, *87*, 2812 – 2824.
[43] EMSL Basis Set Exchange: https://bse.pnl.gov/bse/portal.

